2928-TR1

30 November 1962

FINAL REPORT
ATMOSPHERIC COMPOSITION INSTRUMENTATION

Contract No. 950285 with
California Institute of Technology
Jet Propulsion Laboratory

(SUBCONTRACT UNDER NASA CONTRACT NAS7-100)

HONEYWELL Aeronautical Division

2928-TR1

30 November 1962

FINAL REPORT
ATMOSPHERIC COMPOSITION INSTRUMENTATION

Contract No. 950285 with
California Institute of Technology
Jet Propulsion Laboratory

(SUBCONTRACT UNDER NASA CONTRACT NAS7-100)

Prepared by:

J.E. Crowley
Senior Development Engineer
Advanced Instruments and Display Section

J.G. Ballinger
Senior Research Engineer/Scientist

H.M. Hoeksema
Engineer/Scientist, MPG Research

Approved by: M.P. Dickey

M.P. Dickey
Assistant Project Engineer
Advanced Instrumentation and Display Section

W.H. Bandman/MD

W.H. Boudreau
Section Head
Advanced Instrumentation and Display Section

TABLE OF CONTENTS

LIST OF ILLUSTRATIONS

INTRODUCTION

This is the final report of Atmospheric Composition Instrumentation to measure dewpoint in the atmosphere of Mars. The program was completed in accordance with the JPL Statement of Work, No. SW-2717, dated 21 November 1961, under Contract 950285 between Honeywell and the California Institute of Technology - Jet Propulsion Laboratory. This is a subcontract under Prime Contract NAS7-100 between the Institute and the Government.

SUMMARY

It is generally accepted that the atmosphere of Mars contains water vapor. However, the amount is less than can be detected by present spectroscopic means employing earth-bound instruments. To determine if conditions are suitable for the existence of life, and for a better understanding of certain Martian atmospheric phenomena, knowledge of the vertical distribution of water vapor in the atmosphere is required. Toward this end, early Mars probes will probably carry primary instruments to perform this task. Currently, the best instrument for determining very low concentrations of water vapor during rapidly changing conditions is the automatic frost-point hygrometer. A study has been carried out to define the upper and lower bounds of frost point and atmospheric temperature in the atmosphere of Mars to establish the dynamic range requirements for such an instrument. A bench test model of the instrument was fabricated and was shown to be feasible.

The hygrometer fabricated during the contract consists of a thermoelectric cooler to reduce the temperature of an alpha particle source to the dewpoint temperature. The resulting frost layer on the source material absorbs some of its radiated energy. This absorbtion is measured with a solid-state radiation detector. The frost layer is maintained at a constant thickness by feedback from the detector to the cooler. A thermistor at the source location measures the dewpoint temperature directly.

A study of the temperature and frost point of the atmosphere of Mars indicates that a maximum temperature differential between the thermocooler hot and cold junctions of 91° C permits measurements of frost point at all extremes predicted for Mars.

The instrument was capable of temperature differentials of 50° C and with a three-stage thermocooler will be capable of achieving a delta T of 91° C as required for the worst condition in the Mars atmosphere. The bench test

model consists of a sensing head weighing 1.8 ounces and an electronics section weighing 5.0 ounces. The system has an accuracy of $\pm 0.5^{\circ}$ C. The input electrical power required is 0.4 watt at 24 volts, and 4.5 watts at 1.5 volts. The entire system will withstand sterilization temperatures of 145° C maximum.

SECTION I
TECHNICAL DESCRIPTION

The hygrometer system block diagram is shown in Figure 1. The thermoelectric cooler is a semiconductor. When current flows through the dissimilar conductors, heat is absorbed at the cold junction and evolved at the hot junction. For a given hot junction temperature, the cold junction will have a temperature proportional to the average d-c current. The current may be controlled by varying either amplitude or duty cycle. The device described in this report controls the duty cycle to maintain the cold junction temperature. Figure 2 shows the response of the installed thermocooler to a three-amp step input with the cooler at an ambient temperature of -48° C and at sea level pressure. Figure 3 shows the cooler response at room temperature and at approximately 8 mm of mercury pressure. The response time and delta T of this cooler is less than typical units due to an inefficient heat path from the hot junction to the heat sink.

The polonium 210 source of alpha particles is mounted to the cold junction. The polonium is mounted on a silver foil and is covered with a thin layer of gold. An identical reference source is mounted on an aluminum cylinder maintained at the hot junction temperature. A buildup of frost on the cold junction radioactive source will absorb some of the energy emitted from the polonium. A comparison of the energy emitted from the two sources will determine the variation from normal film thickness.

The radiation detectors are silicon junction alpha detectors packaged in a standard transistor case with a small window at the top of the can. The ionization chamber is a barrier depletion region of a p-n junction formed just below the surface of a small slab of silicon crystal. Alpha particles enter the depletion region and produce electron-hole pairs. The number of pairs increases with the energy of the incoming particle. Output of the detector is a voltage pulse with pulse rate and amplitude proportional to the incoming alpha particle

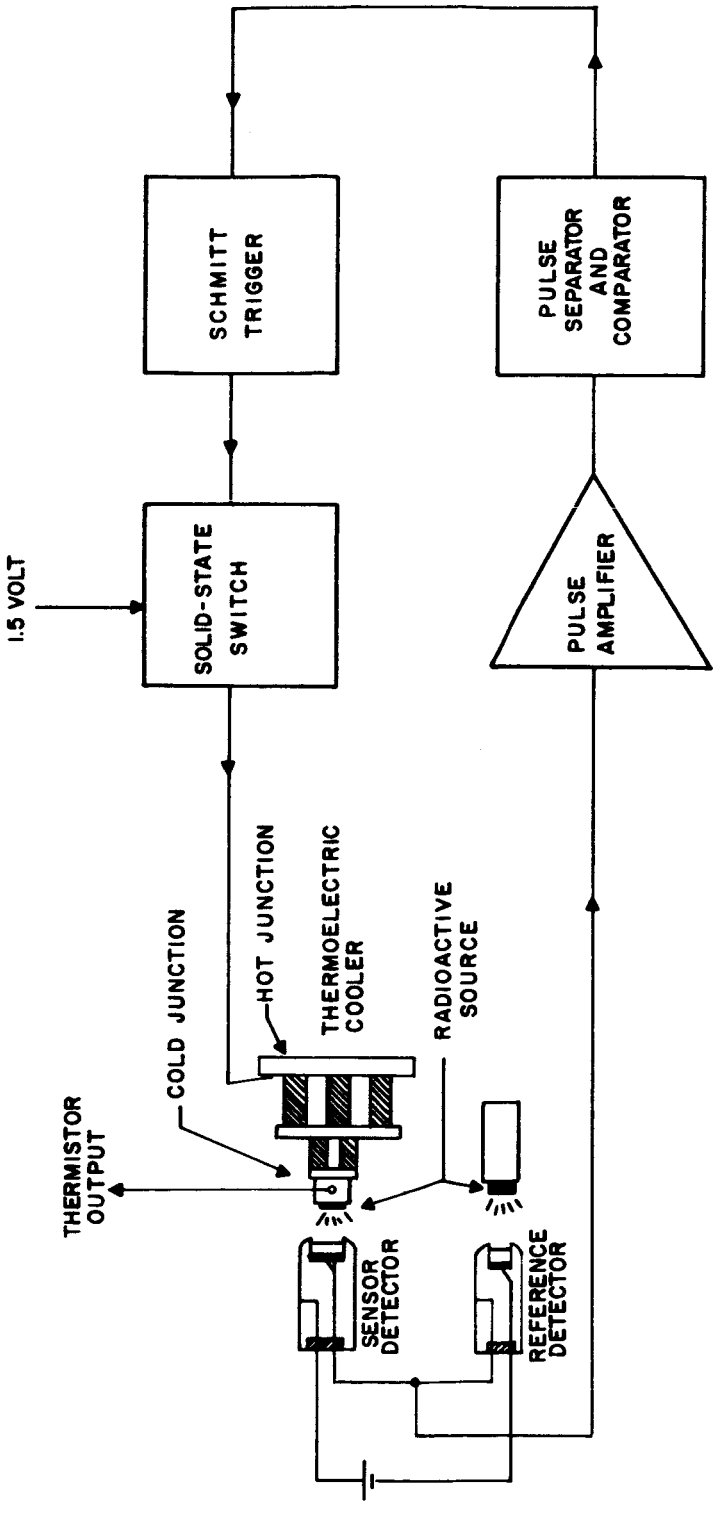

Figure 1. Dewpoint Hygrometer Block Diagram

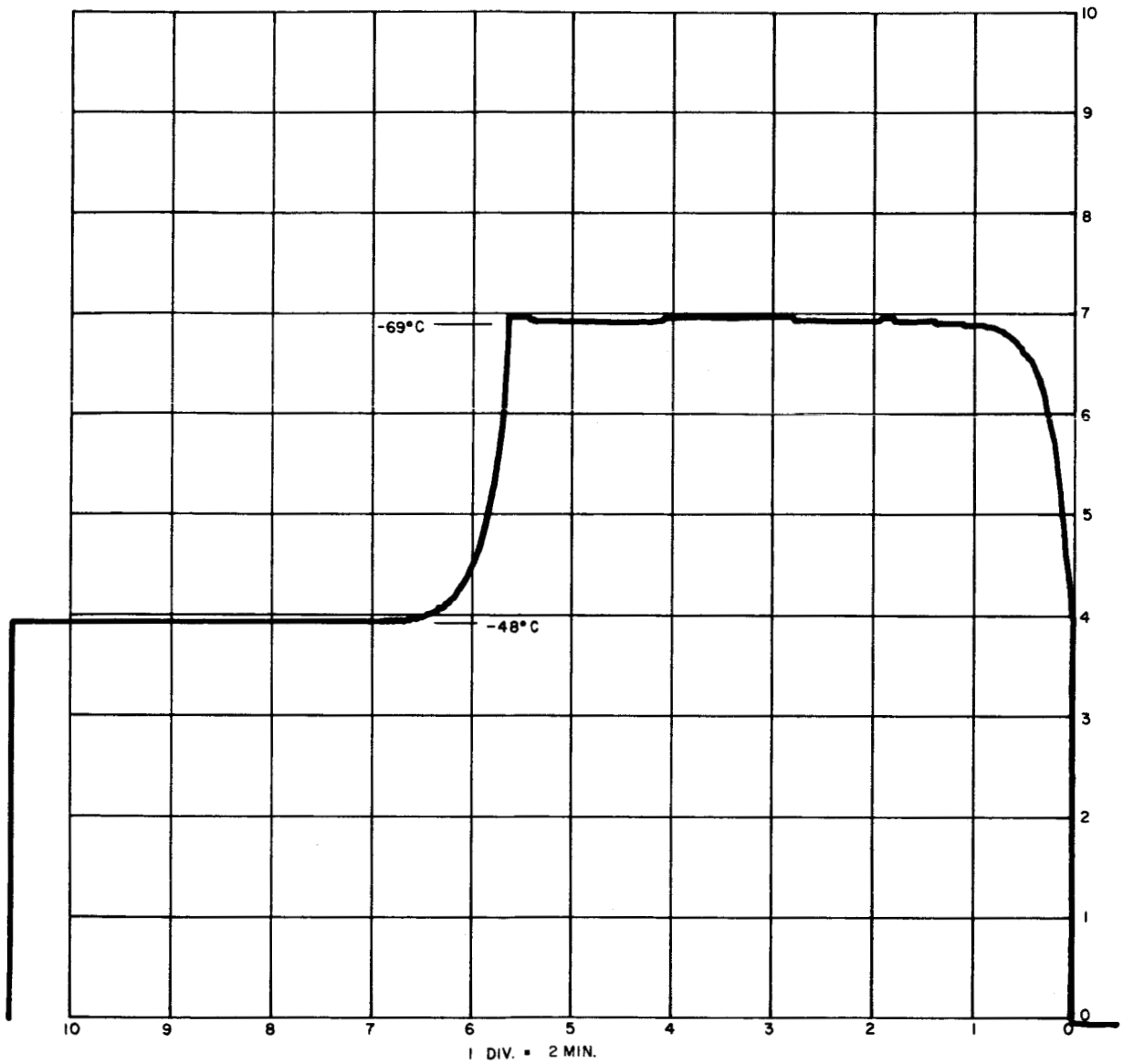

Figure 2. Response of Installed Thermocooler

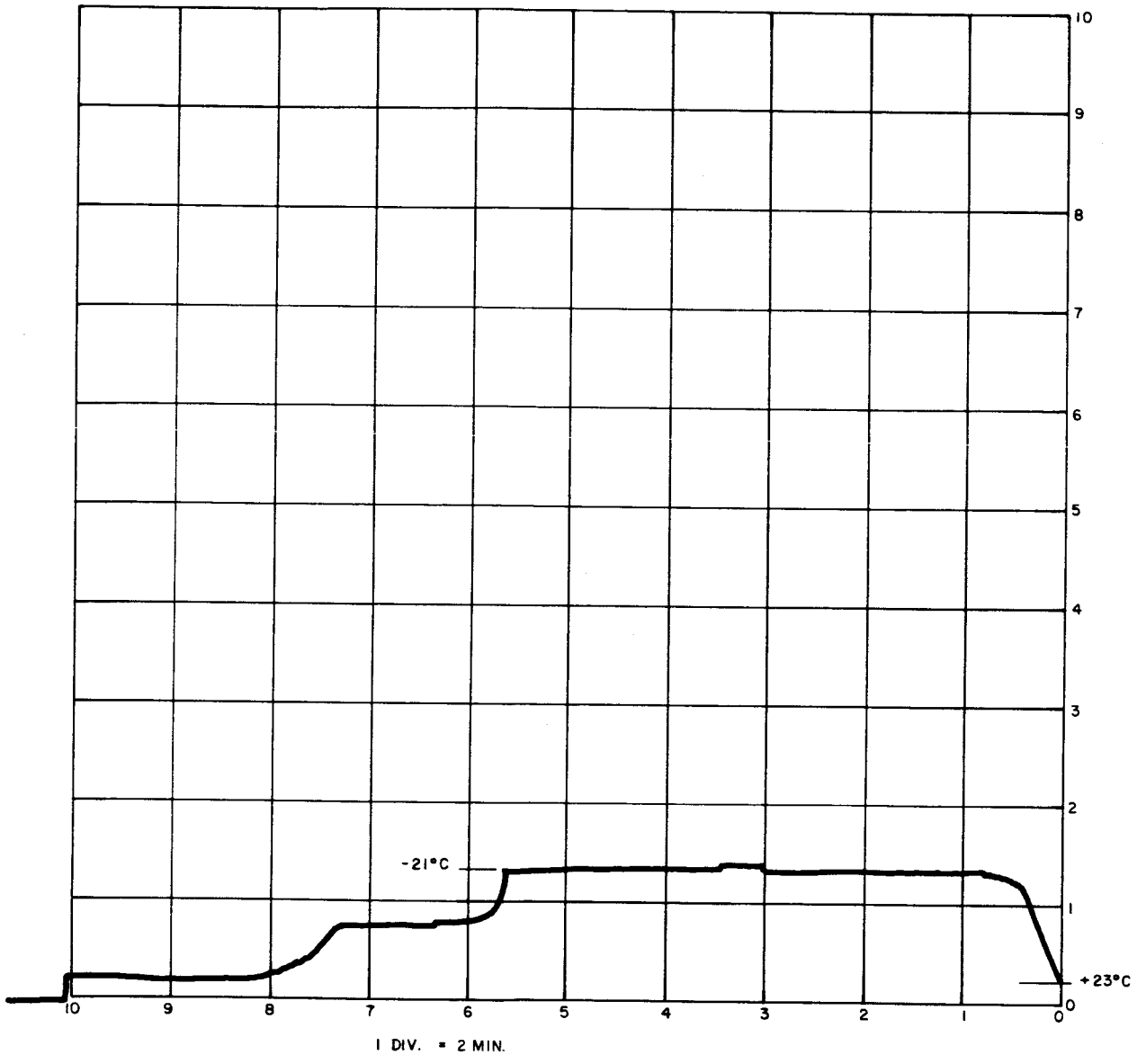

Figure 3. Cooler Response at Room Temperature and Approximately 8 mm Hg Pressure

energy. The sensing detector and reference detector are connected so that the polarities of their pulse are opposing. The two detectors are mounted to the same heat sink and are separated from their respective radioactive sources by equal distances. This cancels all effects of temperature on the detector, effects of air pressure on the alpha particle absorption, and the effect of half-life of the radioactive material.

The detectors, cooler, and alpha particle sources are mounted in a sensing head as pictured in Figure 4. Weight of this head assembly is 1.8 ounces.

The amplifier, pulse separator, comparator, Schmitt trigger, and the solid-state switch are located in the electronics package. This is shown in Figure 5 and weighs 5.0 ounces. The amplifier is a wideband pulse amplifier with sufficient feedback to ensure that both positive and negative pulses are amplified an equal amount. With a linear amplifier, small variations in gain do not affect accuracy as positive and negative pulses are simultaneously affected. The positive and negative pulses are separated with diodes and then integrated. Integrated voltages are compared and the error voltage used to operate the Schmitt trigger. This trigger is then the control for the solid-state switch that energizes the cooler. The entire electronic section consists of nine transistors and requires 17 ma at 24 volts dc. This current can be reduced 50 per cent by changing a Zener diode. This change will be incorporated in any prototype models. The cooler current is 3 amps at 1.5 volts.

The response of the system during closed-loop operation is shown in Figure 6. These curves were obtained by placing the sensing head in an enclosure with silica-gel and then removing the head and exposing it to room environment.

The sensing head, mounted on a heat sink, and the electronic section enclosed in a box for protection are shown in Figure 7. This is the configuration used for all bench model system tests.

Results of hygrometer testing demonstrate that the system can detect changes in frost layer considerably less than 10 micrograms per square centimeter. The thermistor is calibrated to an accuracy better than 0.5 degree centigrade.

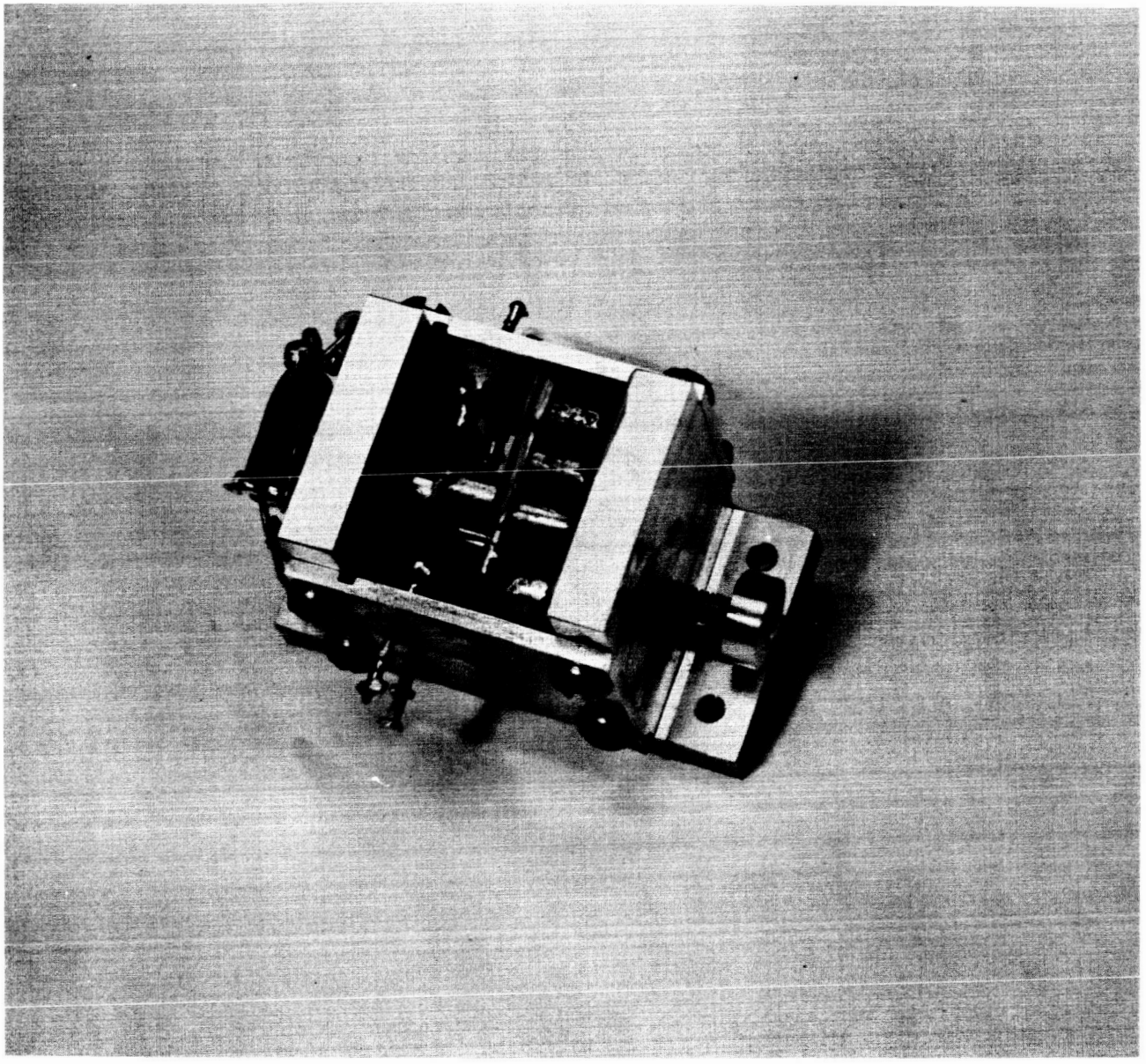

Figure 4. Sensing Head

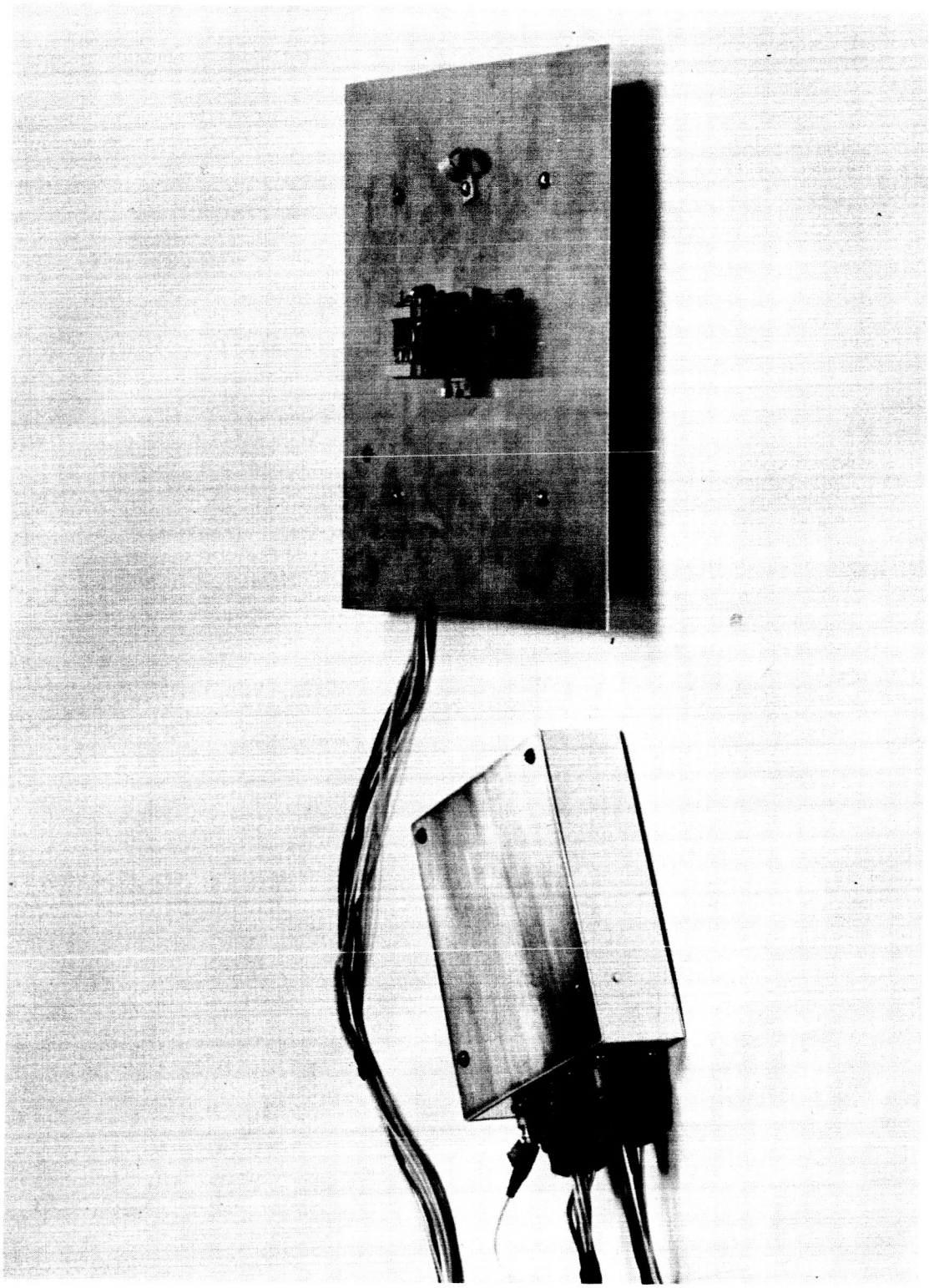

Figure 5. Electronics Section

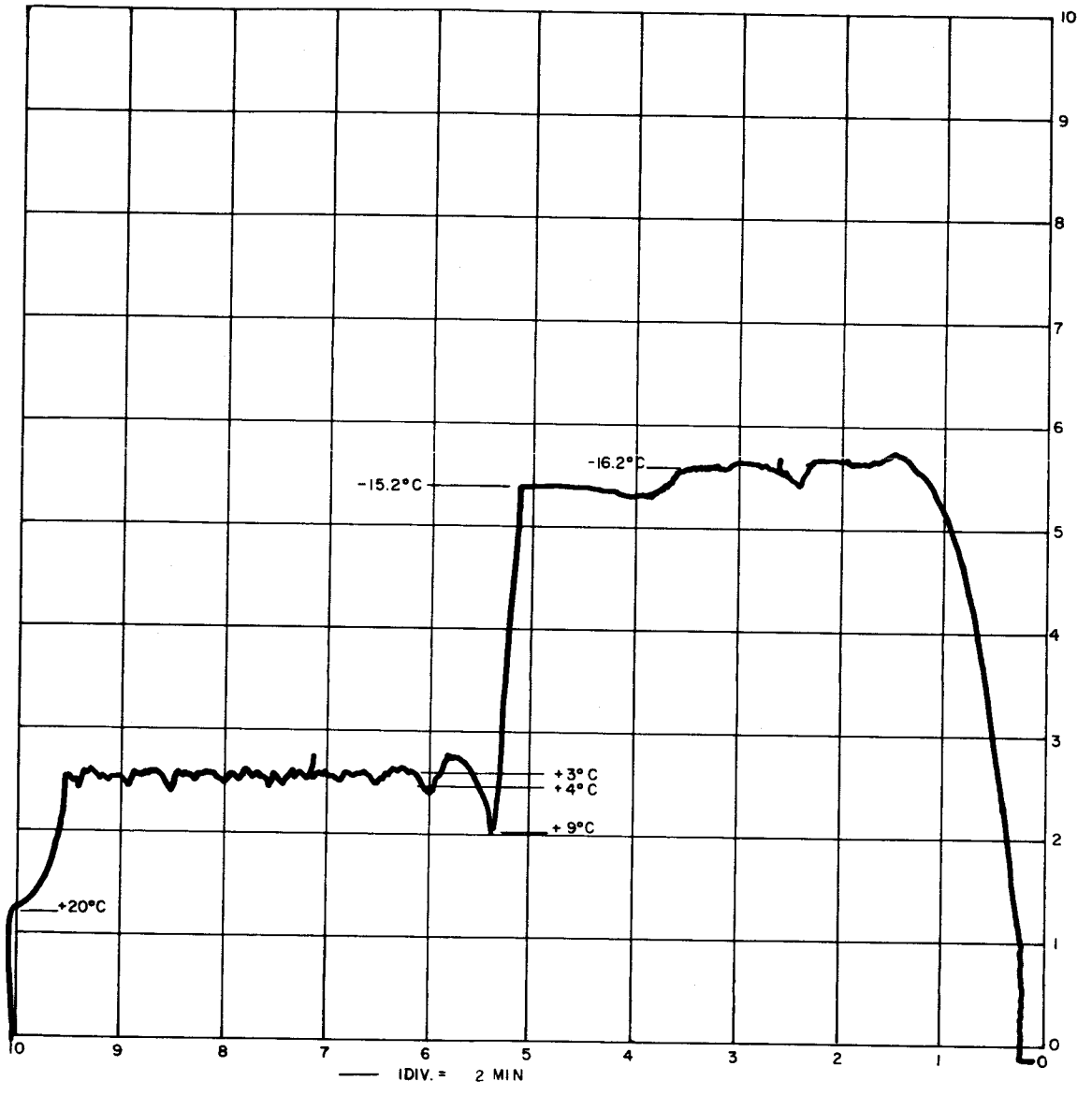

Figure 6. System Response During Closed-Loop Operation

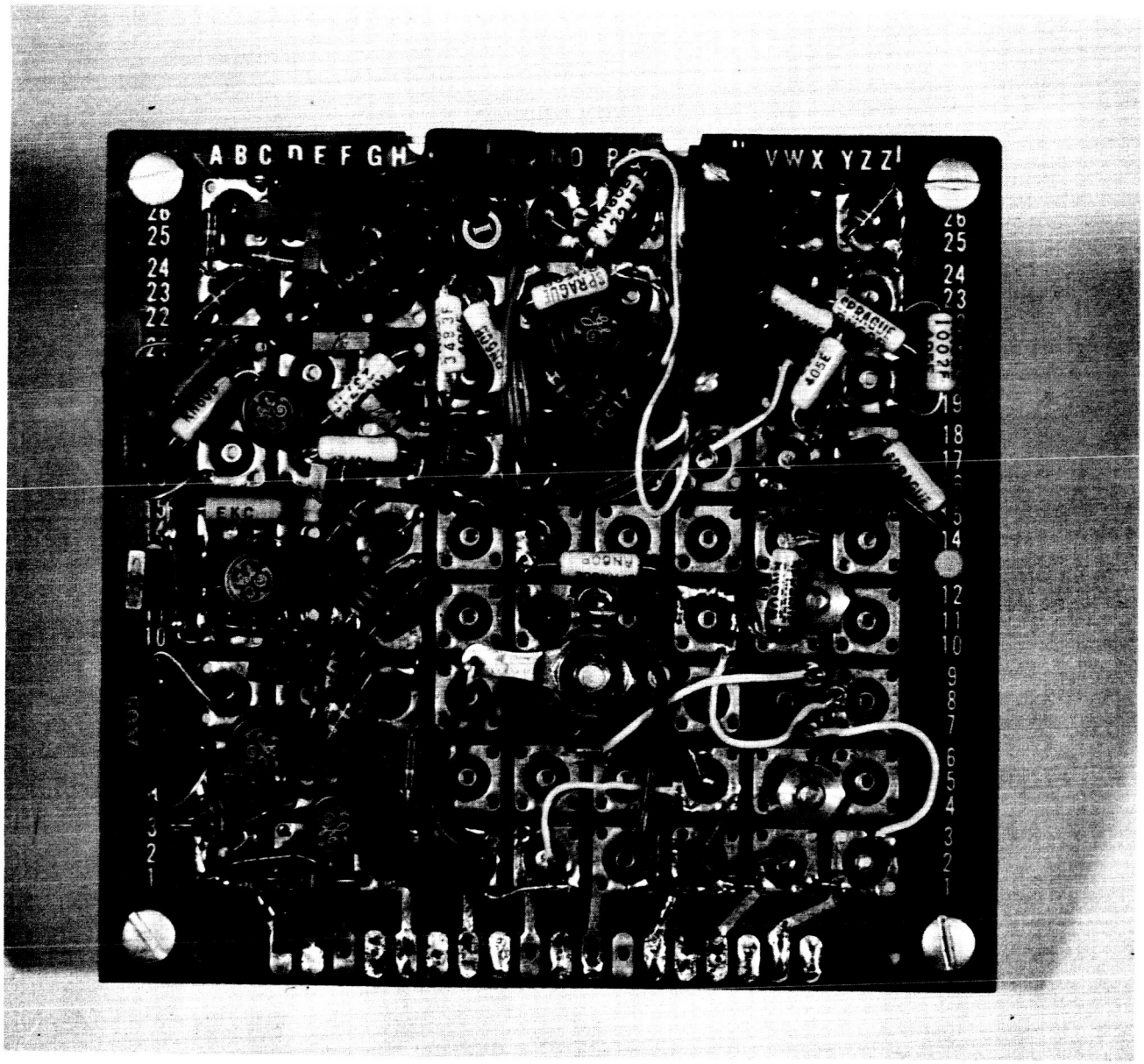

Figure 7. Bench Test System

The system shows no measurable error for variations of pressure and temperature. All parts except the thermocooler have been subjected to 145° C with no change in performance. The thermocooler tested is capable of 125° C operation. A cooler with 145° C capability has been ordered but was not received from the vendor in time to be placed in the unit tested. The alteration necessary in the cooler to convert to high temperature is a change to high temperature solder.

DESIGN INFORMATION

Sensing Head (Bench Test Model)

• Width	1.0 inch
• Height	1.3 inch
• Length	1.7 inch
• Weight	1.8 ounces
• Radioactive source	0.140 diameter foil - polonium 210
• Sterilization temperature	145° C
• Operating temperature range	-90° C to 70° C
• Nominal frost layer thickness	150 ug/cm^2

Electronics (Bench Test Model)

• Width	4.3 inches
• Height	0.8 inch
• Length	4.5 inches
• Weight	5.0 ounces
• Sterilization temperature	145° C
• Operating temperature range	-55° C to 70° C
• Input power	24 volts dc at 0.41 watt 1.5 volts dc at 4.5 watts
• Quantity of transistors	9 (Silicon)

Alternate Electronics with Integral 24 Volts DC to 1.5 Volt DC Converter (Estimated)

• Width	4.3 inches
• Height	0.8 inch
• Length	4.5 inches
• Weight	7.7 ounces
• Sterilization temperature	145^{o} C
• Operating temperature range	-55^{o} C to 70^{o} C
• Input Power	24 volts dc at 6.5 watts
• Quantity of transistors	11 (Silicon)

System Characteristics (Bench Test Model)

• Sensitivity	< 10 ug/cm^2
• Range	See Figure 8
• Response time	$3/4^{o}$ C per second
• Total weight (head plus electronics)	6.8 ounces
• Magnetic properties	less than 1 gamma at 1 foot

THE DISTRIBUTION OF WATER VAPOR IN THE ATMOSPHERE OF THE PLANET MARS

FUNDAMENTAL EQUATIONS

Pressure, Density, and Temperature Distributions in an Atmosphere Having a Constant Lapse Rate of Temperature

Assuming that the temperature T varies linearly with altitude, we can write,

$$T = T_o - \gamma z \qquad (1)$$

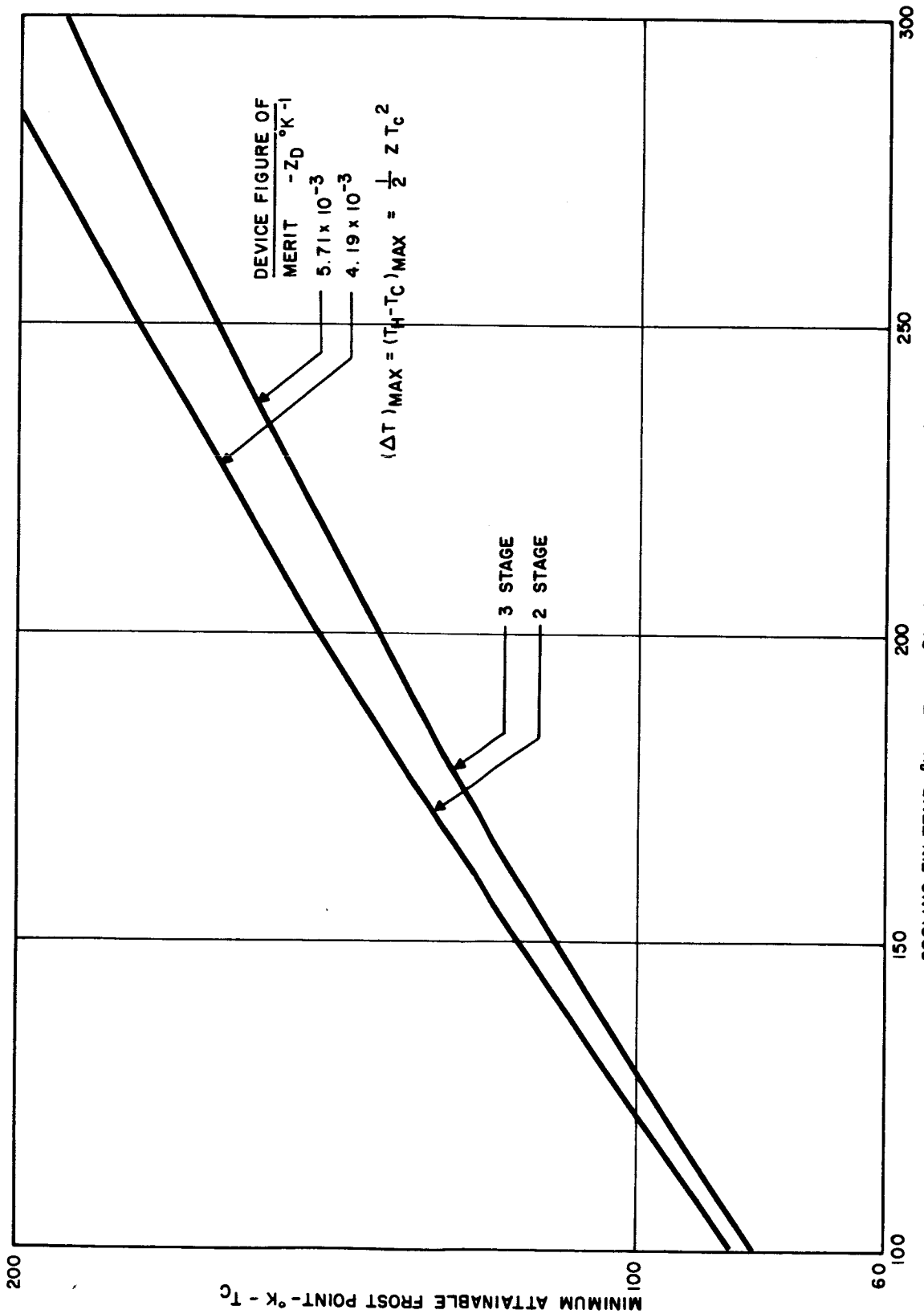

Figure 8. Characteristics of Thermoelectric Modules

where:

T_o is the surface atmospheric temperature

γ is the constant lapse rate of temperature

z is the height above the planet's surface

The hydrostatic equation can be written in the form

$$dp = \rho g \, dz \tag{2}$$

where: ρ is the density

g is acceleration of gravity

With the ideal gas law for dry gases

$$p = \rho RT \tag{3}$$

in which R = gas constant

Equation (2) can be written as

$$dp = -\frac{pg}{RT} dz \tag{4}$$

Integrating Equation (4) yields:

$$p = p_o \left[\frac{T}{T_o}\right]^{\frac{g}{\gamma R}} \tag{5}$$

For an adiabatic process, the first law of thermodynamics yields

$$dw = C_p \, d\,T - \frac{dp}{\rho} = 0 \tag{6}$$

in which C_p is the mean value of specific heat capacity at constant pressure. Combining Equations (2), (3), and (6) yields, for the temperature gradient

$$\frac{dT}{dz} = \frac{g}{Cp} = \Gamma \tag{7}$$

The quantity Γ is called the dry adiabatic lapse rate and it is the maximum gradient which can occur in a free atmosphere. The density at altitude z can be found from the pressure and the ideal gas law,

$$\rho = \rho_o \left[\frac{T}{T_o}\right]^{\frac{C_p}{R}-1} \tag{8}$$

valid for an atmosphere with a dry adiabatic lapse rate.

The Height of the Tropopause Using the Gold-Humphrey's Theory

The stratosphere is assumed in radiative equilibrium with absorbing gas in the troposphere. It receives an infrared flux from the troposphere of σT_t^4 where σ is the Stefan-Boltzmann constant, and T_t is the effective tropospheric temperature. It radiates downward and to space a total flux of $2\sigma T_s^4$ where T_s is the stratospheric temperature.

Since equilibrium exists, we can write

$$2 T_s^4 = T_t^4 \tag{9}$$

HYPOTHESES ABOUT CONDITIONS AND COMPOSITION OF THE MARS ATMOSPHERE

Composition

The only atmospheric constituent which has been identified and measured in the Martian atmosphere is CO_2 (Kuiper, 1952)[1]. Analysis of Kuiper's spectroscopic observations by others, in which the pressure broadening of the absorption lines is taken into account, leads to estimates of 10 to 18 times that present in the terrestial atmosphere. This corresponds to 1.9 to 2.6 per cent by volume.

Except for Kiess (1960)[2] who assumes a Mars atmosphere composed of NO_2 and N_2O_4, it is generally assumed that the major constituent is N_2. Upper limits for minor gases are given under "Frost Point Curves of CO_2, N_2, and Minor Gases".

Pressure, Density, and Temperature as a Function of Altitude

The maximum temperature variation with altitude in a free atmosphere is defined by the adiabatic lapse rate Γ. The value of Γ for Mars is generally accepted to be 3.77° C km^{-1} (3, 1, 4, 5, 6), a value most probable at noon temperatures at the equator.

When, in addition, the effective troposphere temperature T_t is known, we can calculate the tropopause temperature and height above the equator. The value of T_t is estimated from measurements of the atmospheric temperature near the surface and from the lapse rate Γ. deVaucouleur (1952)[5] has summarized the very extensive surface temperature measurements, and concluded that surface temperatures range from 300-318° K as a maximum, 217-230° K as an average, and 160° K as a minimum. Recent measurements by Sinton and Strong (1960)[7] tend to substantiate these values.

Table 1 shows equatorial surface temperatures made by Sinton and Strong[7] in 1954. Figure 9 was derived by Gifford (1956)[8] after temperature measurement made by Coblens and Lampland at the Lowell Observatory. A comparison with measurements of the temperatures in the Gobi desert shows that the temperature of the air above the surface can be considerably lower than the maximum surface temperature. Mintz (1961)[9] calculates a maximum difference of 50° C. Kellogg (1961)[4] assumes then a surface atmospheric temperature near the equator of 220° to 250° K. He uses these figures for the effective troposphere temperatures and derives (through Equation (9)) tropopause temperatures of 210 to 185° K and heights for the tropopause of 11 to 9 km, respectively. Hess (1961)[3] has made a calculation based on a maximum surface atmospheric temperature of 283° K and an average of 217° K. He also assumed the temperature halfway to the tropopause as the effective tropopause temperature and considered lapse rates at different latitudes. He gives a range of possible tropopause altitudes of 27 to 40 km, with temperatures of 182° K to 110° K,respectively. His preferred estimate is a height of 30 to 40 km and a temperature of 140° to 150° K. In addition to the divergence of opinions concerning the surface atmospheric temperature, interpretation of the Gold-Humphrey approximation leads to further discrepancies in temperature estimates, resulting in a 70° C spread at the tropopause. Far better agreement can be observed in the literature concerning the pressure distribution with altitude.

Poisson's equation (Equation (5)) can be applied.

With $\Gamma = 3.7^{\circ}\,\mathrm{C\ km^{-1}}$, $g = 3.75\ \mathrm{m\ sec^{-2}}$

$$R = 0.29\ \mathrm{Joule\ g^{-1}\ {}^{o}K^{-1}}$$

This can be written as

$$p = p_o \left(\frac{T}{T_o}\right)^{3.45} \qquad (10)$$

Table 1. Temperature Dependence on Local Time on Mars

Date	Scan No.	Lateral Degrees	0700 (°K)	0800 (°K)	0900 (°K)	1000 (°K)	1100 (°K)	1200 (°K)	1300 (°K)	1400 (°K)
July 20	5	-2	209	241	257	272	289	295	295	280
20	8	10	209	232	254	271	286	299	301	288
21	9	8	219	238	262	275	291	299	296	293
23	2	14	195	227	252	273	283	289	287	281
23	3	-12	231	241	267	281	291	291	291	281
23	4	-8	218	234	263	282	292	293	293	287

Polarimetric and photometric evidences indicate a surface pressure of 85 mb with a probable error of ± 4 mb (5, 10, 11, 12, 6). The uncertainty in T_o, the surface temperature, introduces a relatively small error in the estimates of the pressure distribution. In the same way, the density distribution with height can be found with Equations (8) and (3).

$$\rho = \rho_o \left(\frac{T}{T_o}\right)^{2.45} \qquad (11)$$

The pressure and density curves are shown in Figure 10.

Estimates as to the Amount of Water Vapor in the Mars Atmosphere

Water vapor has not been detected spectroscopically in the atmosphere of Mars. The upper limit for the amount of water vapor is therefore defined by the sensitivity of the spectrometer. A value of 3.5×10^{-2} gm cm^{-2} given by Dunham (1952)[13] is generally accepted. This is the total mass of water vapor above 1 cm^2 in the Mars atmosphere.

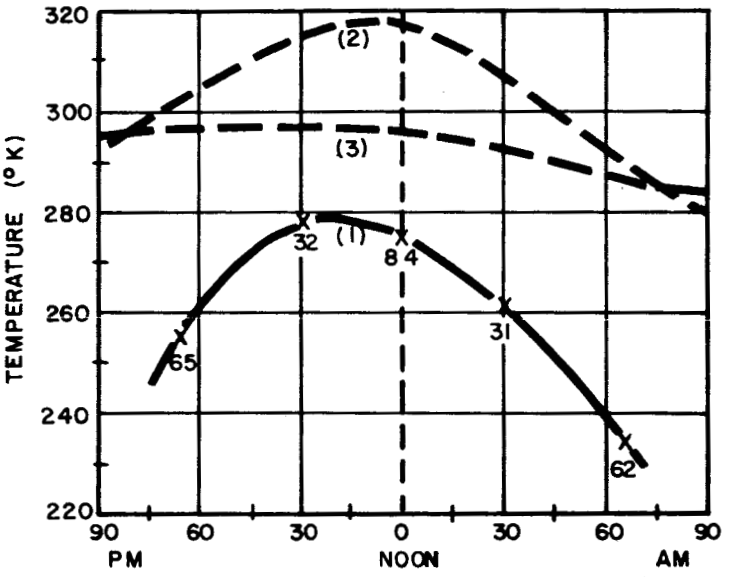

Figure 9. Average temperature variation near the Martian equator, i.e., the diurnal temperature variation: horizontal coordinate is degrees longitude east or west of the noon meridian; the number of individual observations averaged at each point is indicated; 2 and 3 are Haude's observations of the diurnal temperature variation at, respectively, zero and 2 meters above the Gobi Desert in June.

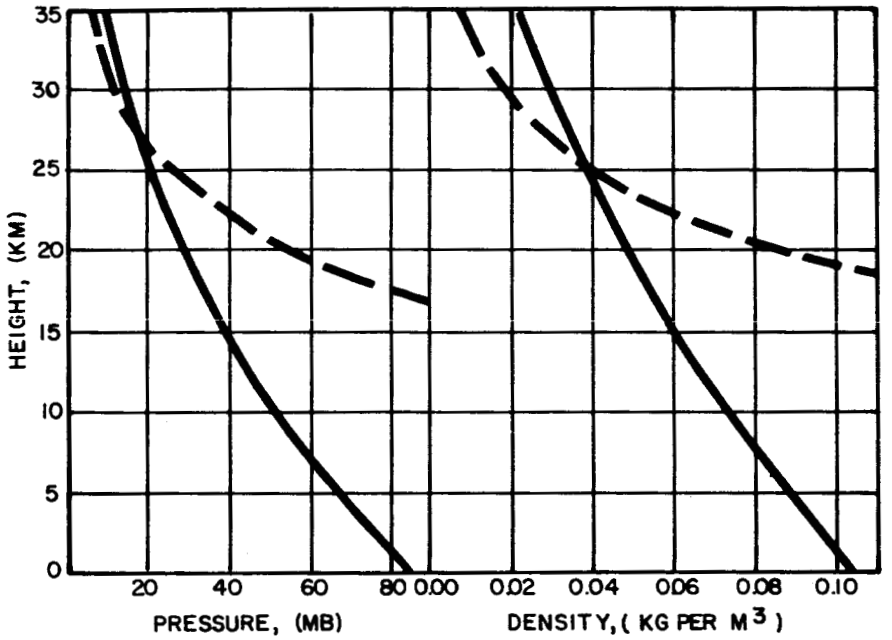

Figure 10. The variation of pressure (left) and density (right) with height in the atmospheres of Mars (solid lines) and earth (dashed lines). The Martian curves are for an adiabatic lapse rate of temperature assuming $T_o = +10^o$ C, $p_o = 85$ mb. The terrestrial data are for the NACA Standard Atmosphere.

Evidence of the presence of water vapor are the measurements of the reflection spectrum of the polar caps by Kuiper (1952)[1], which is similar to that of frost at low temperatures, and measurements by Dollfus(1951)[14] of the polarization of the caps which is also the same as that of frost at low temperatures. In addition, white clouds observed over the polar caps and at the limbs* and the blue haze** are often explained as consisting of small ice particles.

Sagan (1961)[15] shows that the amount of CO_2 which is detected spectroscopically is not sufficient to explain the Greenhouse effect*** which gives a discrepancy of 30^{o} K between theoretical radiation temperature and the observed thermocouple temperature of Mars. With the vapor pressure above the caps, temperature, and the Greenhouse effect, he finds through iteration an approximate value of 10^{-2} gm cm^{-2}, for the amount of water vapor and a lower limit of 10^{-3} gm cm^{-2}.

The per cent by volume of water vapor in the Mars atmosphere is approximately equal to the mass ratio times the ratio of the gas constants. Using estimates of the total mass of the Mars atmosphere, which range from 200 gm cm^{-2} (16, 12, 17) 227 gm cm^{-2} (6) to 300 gm cm^{-2} (18), we find the upper and lower limits of volume ratio to be:

$$V = \frac{10^{-3}}{300} \times \frac{4.6}{2.9} \times 100 \text{ per cent to } \frac{3.5 \times 10^{-2}}{200} \times \frac{4.6}{2.9} \times 100 \text{ per cent}$$

$$= 5.3 \times 10^{-4} \text{ to } 2.9 \times 10^{-2} \text{ per cent}$$

*The limb or terminator is the line dividing the illuminated and the unilluminated part of a planet's disk.

**A blue haze in the Mars atmosphere is generally considered to be responsible for the fact that photographs of Mars taken in blue, violet, and ultraviolet light show less detail than those taken in yellow, red, or infrared light.

***The Greenhouse effect is the property of an atmosphere of being transparent to light rays but rather opaque to infrared rays, just as the glass in a florist's greenhouse. It acts as a trap for heat, raising the temperature inside by many degrees.

Urey (1957)[6] gives $2.9.10^{-2}$ per cent Makemson (1961)[19] gives 3.10^{-2} per cent. An even lower value than the lower limit of 10^{-3} gm cm^{-2} given by Sagan (1961)[15] is 2.10^{-4} gm cm^{-2} derived by Hess (1961)[3] in his explanation of the blue haze. At certain periods, this violet or blue layer clears and the surface becomes visible. Kuiper (1952)[1] and Hess (1961)[3] made calculations showing that this haze layer can consist of small ice particles. Other opinions as to the cause of the blue haze have been advanced by other authors, (17, 20, 18, 11, 21, 22, 23). Hess (1961)[3] assumes the thickness of the layer to be 3 km.

Assuming a constant mixing ratio, the frost-point curve of water vapor will be approximately a straight line. The haze layer which covers the whole planet can then only appear at the base of the tropopause as is shown in Figure 11. With the height of the cloud base at 29.3 km, the surface frost point has to be 183^{o} K and the precipitable water content 2.10^{-4} gm cm^{-2}.

Proposed Frost-Point Profiles

Hess (1958)[16] states that in an adiabatic atmosphere complete mixing of all constituents occurs, so that the proportion of H_2O to the remainder of the constituents remains constant with height. The earth's atmosphere is considered to be in adiabatic equilibrium. However, on earth the frost-point (or dewpoint) curve follows roughly the air temperature curve which leads to a sharp decrease in mixing ratio up to the tropopause. Also, over desert regions, experiments have shown that approximately the same decrease in mixing ratio holds. It is very likely that a similar effect appears in the Mars atmosphere since there is a similarity of weather phenomena.

"There is a preponderance of processes which concentrates the water vapor in the very lowest portion of the atmosphere" (Hess, 1948)[24]. Similar remarks have been made by deVaucouleur (1952)[5] and Focas (1962)[25]. In his discussion of the blue haze, Hess (1961)[3] calculates a water vapor content of 2.10^{-4} gm cm^{-2} and a surface frost point of 183^{o} K, assuming a constant mixing ratio. In another article, Hess (1948)[24] derives a water vapor content of 4.10^{-2} gm cm^{-2} assuming

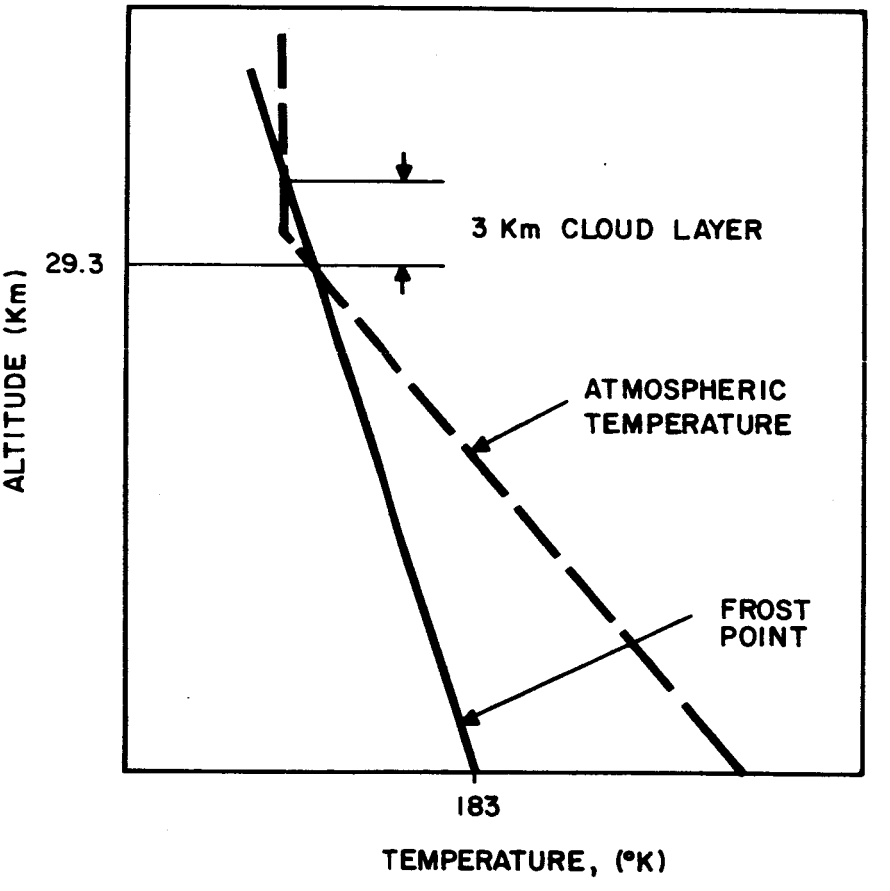

Figure 11. Temperature Versus Attitude

that the water vapor is concentrated in a layer of 0.5 km thick. In the latter calculation, he uses the upper limit of temperature of 253° K given by Coblens and Lampland for the temperature at the sunrise limb during the time that a haze occurred.*

The first value of 2.10^{-4} gm cm^{-2} is lower than the range suggested in literature. The second value of 4.10^{-2} gm cm^{-2} is higher than this range.

As we see, there is a wide range of frost-point curves suggested in literature, each of them explaining a different phenomenon in the Mars atmosphere.

It appears desirable to use a different approach and use as a basis for our calculations the estimates for total water vapor content as given by Sagan[15].

The similarity of atmospheric conditions on earth and on Mars will allow us to define an upper limit for the variation in mixing ratio with height. On earth, it is known that except for deviations due to disturbances such as cloud formations, etc., the maximum gradient of the frost-point curve is the same as the maximum gradient of the temperature curve. It we postulate that the same holds for Mars, then the maximum gradient of the frost-point curve is 3.7° C/km. In Figure 12, frost-point curves are drawn with this gradient starting at surface temperatures with intervals of 10° C. As a parameter, the total water vapor content above 1 cm^{-2} in Mars atmosphere is given. This is calculated as follows: From the frost point at a certain height, the vapor pressure is known. The density can be found from the gas law in which we assume that the temperature of the atmosphere is that above the equator at noontime (lapse rate 3.7° K/km).

---

*White or blue clouds may be observed on any part of the disc but are concentrated toward the limb. Angular sizes up to 45° in areo graphic coordinates (about 3000 km) extending along the limb are observed. On the morning side of the disk, clouds may extend almost to the noon meridian, on the afternoon side rarely over 65° from the terminator[26].

The fact that these clouds are frequently found on the sunset or sunrise terminators, suggests strongly that the clouds are due to condensation, for the rapid change of temperature which must take place at sunset and sunrise is the only obvious reason for clouds to form in these particular places.[11]

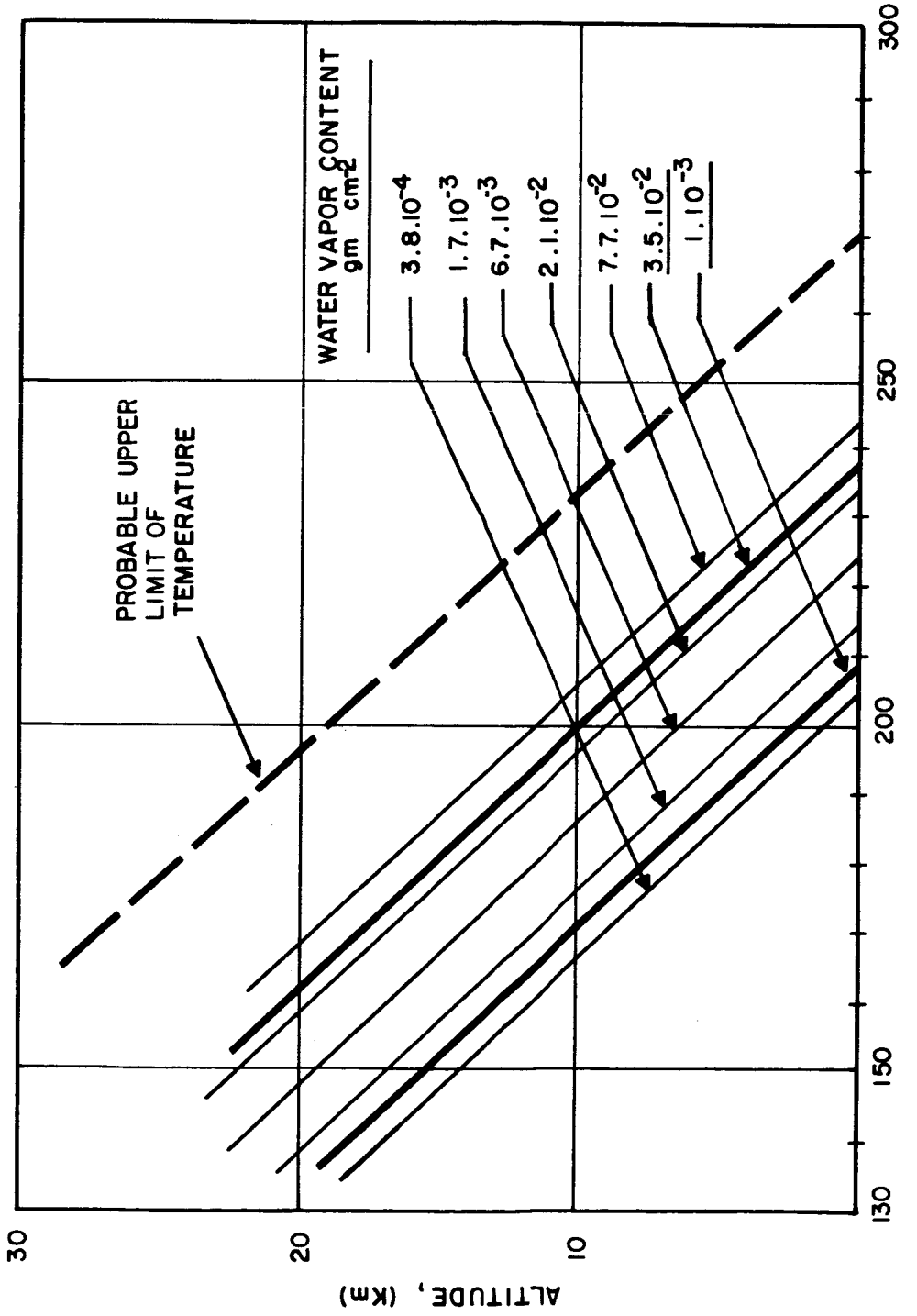

Figure 12. Frost Point at Various Surface Temperatures

The density curve is plotted and integrated. For this calculation we neglect the content above the point where the density is 10^{-3} times the surface density for water vapor. The latter point is within 10 km, or below the tropopause. It is therefore not necessary yet to define the height of the tropopause.

Through interpolation we find the frost-point curves for 10^{-3} gm cm^{-2} and $3.5.10^{-2}$ gm cm^{-2}.

In Figure 13 two sets of frost-point curves are given; one set consists of the above found upper and lower limit of frost point for the upper limit of decrease in mixing ratio. The other set comprises the possible range of frost-point curves for a constant mixing ratio.

The maximum surface atmospheric temperature (noontime at the equator) is assumed to be 283^{o} K (1, 3). With a diurnal variation of surface temperature from 200 to 318^{o} K, this value is certainly the upper limit.

As we discussed before, the frost-point curves derived with constant mixing ratio fail to explain the existence of low level clouds. The frost-point curves derived with the extreme variation of mixing ratio with height do not intersect with the atmospheric temperature and thus cannot account for the existence of small ice particles at high altitudes. Both of these phenomena could be explained if we were to consider a variation of mixing ratio with height which lies between these two extremes.

As an example, we chose a total water vapor content of $1.6.10^{-2}$ gm cm^{-2} which is a likely value based on the literature. With this, we can draw a frost-point curve as shown in Figure 14a. In Figure 14b, the mixing ratio as a function of altitude is drawn. The atmospheric temperature curve is assumed to start at a surface air temperature of 270^{o} K and having a lapse rate of 3.7^{o} C/km. These curves show:

- A blue haze and the tropopause at an altitude of approximately 30 km at a temperature of about 160^{o} K which is in close agreement with these estimates.

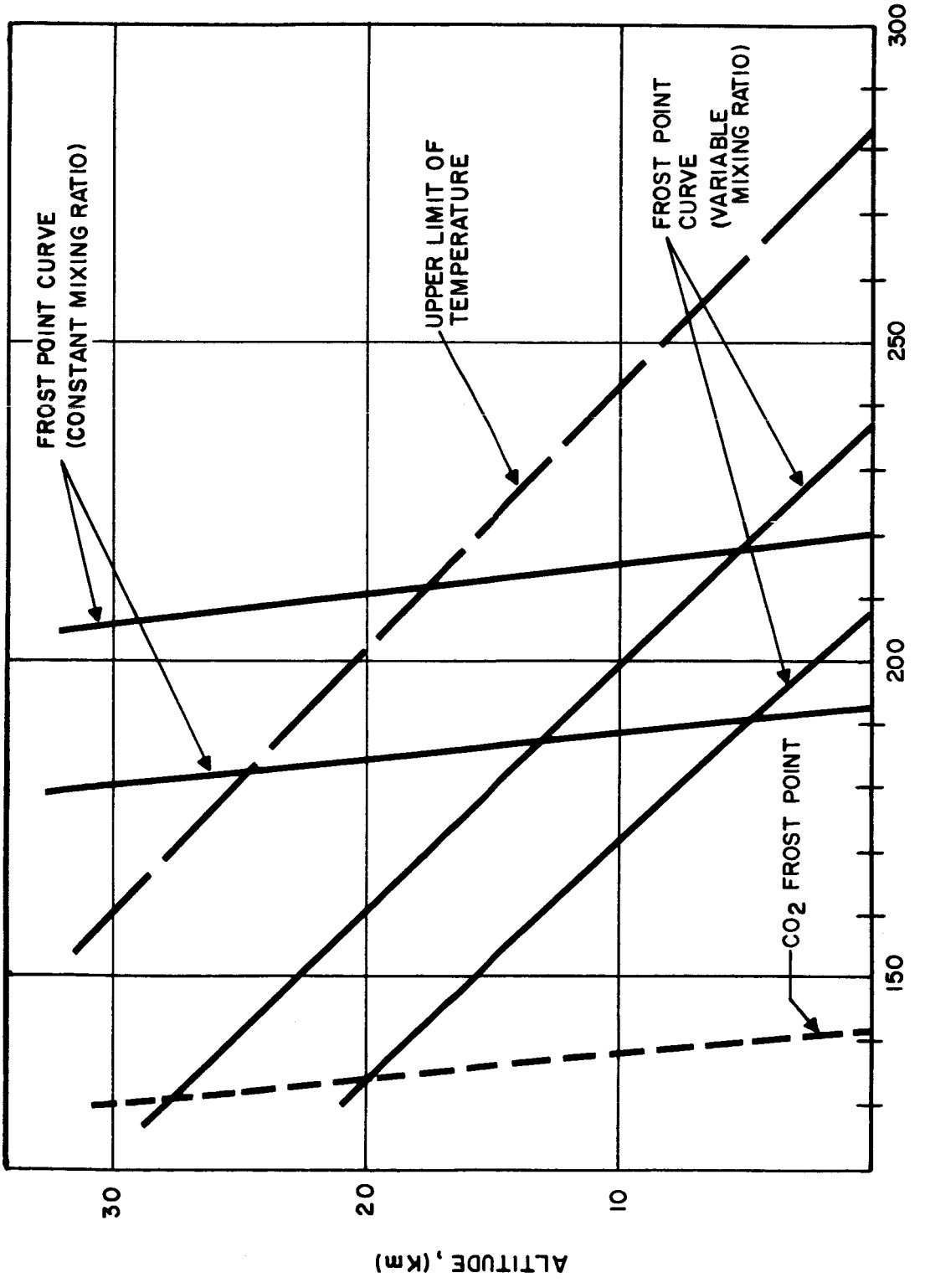

Figure 13. Frost Point Curves

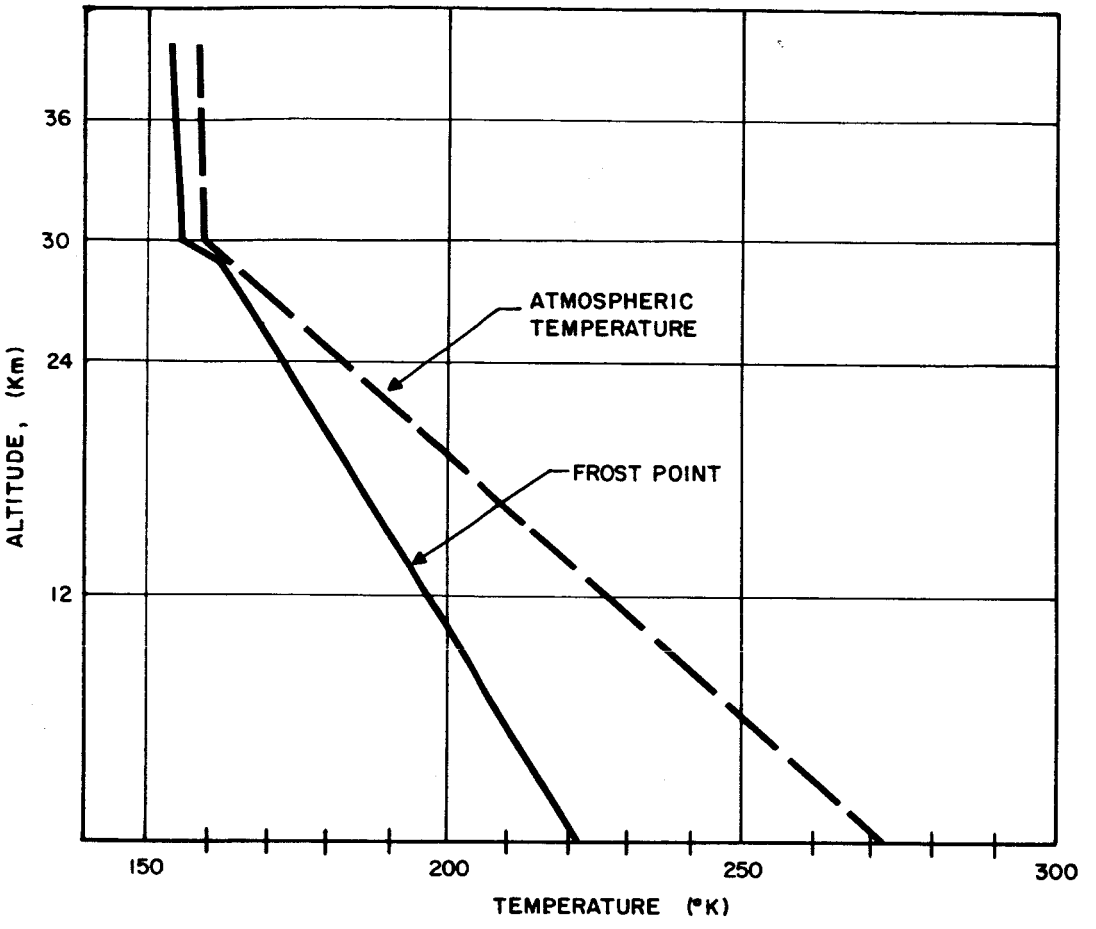

Figure 14a. Temperature versus Altitude

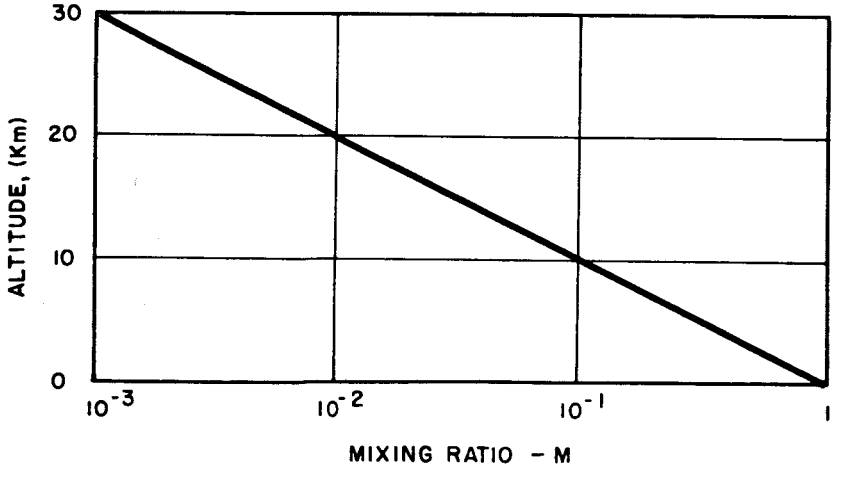

Figure 14b. Mixing Ratio versus Altitude

- A surface frost point of -50° C. This value is lower than the measured surface temperature during haze and cloud formation. However, as Gifford (1956)[8] and Mintz (1961)[9] pointed out, the atmosphere above the surface in equatorial regions has a much lower diurnal variation in temperature than the surface itself and with reported night temperatures of -70° C at the equator[7], a surface frost point of -50° C is easily possible.

- The polar caps are formed when the temperature drops below -50° C.

FROST-POINT CURVES OF CO_2, N_2, AND MINOR GASES

Except for CO_2, none of the gases mentioned below have been detected spectroscopically. Kuiper (1952)[1] has estimated the upper limits for N_2, A, CO_2, O_2, SO_2, N_2O, CH_4, C_2H_4, C_2H_6, and NH_3. Also, upper limits for NO_2 and N_2H_4 have been set up by Kaplan (1961)[27] and Sinton (1961)[28], respectively. These limits are usually given in cm atmosphere*.

For the purpose of converting these to frost points, the upper limits are given as volume per cents. The absolute pressure at the surface is taken as 90 mb and at a height of 30 km as 16 mb. Frost points of the major and minor gases are given in Table 2.

*The unit cm atmosphere is a measure of the amount of gas contained in a column of arbitrary length, pressure, and temperature. It is the path length in cm containing the same number of molecules as the arbitrary column which the gas would occupy if it were reduced to N.T.P.

Table 2. Frost Points of Major and Minor Gases

Gas	Upper Limit of Volume %	Frost Point at 0 km °K	Frost Point at 30 km °K
CO_2	3	142	133
N_2	95	62	57
A	3	57	51
SO_2	$1.72.10^{-6}$	115	109
O_2	$1.37.10^{-1}$	40	45
N_2O	$1.13.10^{-1}$	118	110
CH_4	$5.62.10^{-3}$	52	47
C_2H_4	$1.13.10^{-3}$	74.3	70.1
C_2H_6	$5.62.10^{-4}$	83.0	79.8
NH_3	$1.13.10^{-3}$	125	120

CONCLUSIONS

With respect to the measurement of the vertical distribution of water vapor in the atmosphere of the planet Mars by means of a frost-point hygrometer, the following remarks may be made.

- It is certain that frost-point curve and atmospheric temperature curve sometimes intersect at low altitudes.
- It is very likely that they intersect at higher altitudes.
- To confirm the blue haze theory, the instrument should be capable of measuring frost points, which may be as low as 168^{o} K.

- The temperature difference between the atmospheric temperature and the frost point may be small for all latitudes and times except near noon at the equator.

- The frost-point curves of all other major and minor gases will be below the frost-point curves for water vapor in the altitude range of interest.

- In the case of an atmosphere consisting of oxides of nitrogen as postulated by Kiess (1960)[2], the hygrometer will track a frost point which starts at 253° K at the surface. As we see from Figure 13, the maximum surface frost point for water vapor can be no greater than 237° K which should make it possible to determine which of these the hygrometer has been tracking.

- A lower limit of atmospheric temperature is set by the fact that there can be no condensed CO_2 in the atmosphere (Hess, 1961)[3]. Frost points of water vapor lower than the possible frost point of CO_2 which could in the extreme case occur above 20 km are beyond the altitude range of interest. Thus the upper limit of CO_2 frost points is the lower limit of the range of the hygrometer.

- From Figure 13 we can define the lower limits of frost points with the corresponding atmospheric temperature. A safe range for the hygrometer is:

  Frost points from 139° K-191° K with $0<\Delta T<75^{\circ}$ K

  Frost points from 191° K-190° K with $0<\Delta T<91^{\circ}$ K
  where ΔT is the difference between frost point and the atmospheric temperature.

It should be noted that these are extreme ranges, where ΔT_{max} is based on temperatures over a relatively small area of the planet (near the equator) and, at a time when the temperature is highest (around noontime). This means that even in the case that these extreme conditions exist, the chance of encountering these conditions is very small.

SECTION II
POST DESIGN CRITIQUE AND RECOMMENDATIONS

The aims of further improvement of the present bench test model are the input voltage and current requirement, the delta T, and the speed of response.

The present input power is 24 volts at 17 ma and 1.5 volt at 3 amps. A circuit change to a zener diode with a test current of two ma instead of the present 10 ma will reduce the 17 ma to 9 ma. This was not done on the bench test model because of delivery schedules. A d-c to d-c converter would eliminate the necessity of a 1.5 volt supply and under such an arrangement the input required would be 24 volts at 270 ma. This converter would add 2.7 ounces to the system weight.

The delta T and response time of the bench test model are shown in Figures 2 and 3. However, the cooler used in this model was a new design and is operating at only 60 percent of the delta T specified by the vendor for the three amp driving current. Thermocooler types being used on Honeywell balloon models have about 25 percent of the response time measured on the bench test model.

These discrepancies are caused by faulty coolers, poor heat conduction to the heat sink, or too large a mass on the cold junction. These effects are being investigated by the vendor and by Honeywell. Improved models should be available in the near future.

All previously described problems (delta T, power, and response) are functions of the thermocooler. Emphasis will be placed on thermocooler improvements during future Honeywell development programs. The application of thermocoolers in the dew point hygrometer is different from most present cooler design applications. Most coolers are now designed to pump the heat from an electrical load to cool electronic components. Speed of response and power requirements are not important considerations in such

applications. Thermocoolers especially designed for the hygrometer should result in considerable improvement of the present limitations because the thermal efficiency of the cooler would be increased.

The delta T of a thermocooler is proportional to current so that some compromise will always be necessary between maximum delta T and power. The maximum delta T of 91° C in the Mars atmosphere occurs on a limited portion of the planet during a specific hour of the day. Some consideration should be given to the probability of landing under such conditions. If this probability is very small a lower maximum delta T should be used as a design specification in order to reduce power requirements.

The thermocooler could be eliminated if a heat of fusion heat sink were used. However, this would create the problem of freezing the material during the transit period.

The basic advantages of the Honeywell hygrometer are no moving parts, stable calibration, high sensitivity to change in frost layer thickness, continuous readings, accuracy, and a large range because the device maintains a temperature differential between the heat sink and cold junction. (Dew point is low at low ambient temperatures and the minimum measurable dew point is decreased as the heat sink temperature is lowered). The hygrometer sensitivity is increased at low pressures because the thermal efficiency is increased. It is recommended that the next phase of the hygrometer study include the following items:

1. Test of present bench test model during a high attitude balloon flight to obtain operational characteristics under conditions approaching the Mars environment. Prior to this flight, the instrument would be calibrated in a "two pressure" humidity chamber having an accuracy of $\pm$ 0.1° C. The "two pressure" principle involves saturating air with water vapor at an elevated pressure and expanding it isothermally to the pressure of the test chamber. The ambient temperature range of the Honeywell two pressure system is -40° C to 50° C.

2. Subject the present bench test model to an accelerated life test by storing at an elevated temperature of 100° C for forty-five days. This test will indicate the effect of component aging during the transit portion of the Mars flight. Periodic periods under vacuum during this test will determine if migration of the radioactive material will contaminate the detector.

3. A study of thermocoolers to determine the best compromise of input power, delta T, and time constant. Various types of construction should be tested during this study. The study should be made at various temperatures and pressures.

4. A continued study of heat sink design to improve the cooler time constant.

5. An investigation of the effects of various frost layer thicknesses on response and sensitivity.

6. An investigation of ventilation rates to determine their effect on dewpoint tracking.

7. Specifications for delta T, tracking rates, environment, and preliminary packaging configuration will be prepared to form the requirements of a prototype model.

8. Fabrication of a prototype model to the specification of Item 7 incorporating improvements that result from Items 1 through 6.

9. Testing of the prototype model to determine effect of voltage variations, tracking rates, temperature, pressure, and sterilization baking. These tests should include actual balloon flights of the system.

REFERENCES

1. Kuiper, G.P., 1952, "The Atmospheres of the Earth and Planets", University of Chicago Press.

2. Kiess, C.C., Karrer, T., and Kiess, H.K., 1960, "A New Interpretation of Martian Phenomena", Pub. of the Astron. Soc. Pacific, V. 72, p. 256-267.

3. Hess, S.L. 1961, "Mars as an Astronautical Object", in Advances in Space Science and Technology, Vol. III.

4. Kellogg, W.W., and Carl Sagan, "The Atmospheres of Mars and Venus", A report by the ad. hoc. panel on planetary atmospheres of the science board, 1961.

5. deVaucouleur, G., 1952, "Physics of the Planet Mars".

6. Urey, H.C., 1959, "The Atmospheres of the Planets", p. 363-415 in Encyclopedia of Physics, V. 52, Astrophysics III. The Solar System, S. Flugge, ed., Springer-Verlag, 601 pp.

7. Sinton, W.M., and Strong, J., 1960, "Radiometric Observations of Mars", Astrophys. Journal, Vol. 131, pp. 459-469.

8. Gifford, F., 1956, "The Surface Temperature Climate of Mars", Astrophys. Journal, V. 123, p. 154-161.

9. Mintz, Y., "A Note on the Temperature of the Equatorial Troposphere of Mars", in Studies of the Physical Properties of the Moon and Planets, Quarterly Technical Progress Report (3),Contract RM-2769-JPL, The Rand Corporation, p. 81, 1961.

10. Grandjean, J., and Goody, R.M., 1955, "The Concentration of Carbon Dioxide in the Atmosphere of Mars", Astrophys. Journal, V. 121, p. 548.

11. Goody, R.M., 1957, "The Atmosphere of Mars Weather", V. 12, p. 3-15.

12. Dollfus, A., 1948, "Polarization Study of the Light Reflected by Clouds and the Atmosphere of the Planet Mars", Comptes Rends,V. 237, p. 383.

13. Dunham, T., 1952, in The Atmospheres of the Earth and Planets, G.P. Kuiper, ed., University of Chicago Press, p. 299.

14. Dollfus, A., 1951, "The Polarization of Light from the Different Regions of the Surface of Mars and Its Interpretation", Comptes Rends, V. 233.

15. Sagan, Car, "The Abundance of Water Vapor on Mars", Astrophys. Journal, V. 66, p. 521, 1961.

16. Hess, S.L., 1958, "Blue Haze and the Vertical Structure of the Martian Atmosphere", Astrophys. Journal, V. 127, p. 743.

17. Briggs, M.H., and Revill, J.P., 1960, "The Chemistry of Mars, I.", "The Atmosphere", Journal of the Brit. Interplanet. Soc., V. 17, p. 391-393.

18. Opik, E.J., 1960, "The Atmosphere and Haze of Mars", Journal of Geophys. Res., V. 65, p. 3057-3063.

19. Makemson, M.W., Baker, R.N.L., Jr., and Westrom, G.B., "Analysis and Standardization of Astrodynamic Constants", University of California, Astrodynamical Report No. 12.

20. Went, F.W., 1960, "Blue Hazes in the Atmosphere", Nature, V. 187, p. 641-643.

21. Rosen, B., 1953, "Possible Origin of the Violet Layer in the Mars Atmosphere", Ann. d'Astrophysique 16, 1953.

22. Sharonov, V.V., "On the Role of True Absorption in the Martian Atmosphere", Soviet Astronomy 1, 547-556, April, 1957.

23. Guerin, P., "Spectrophotometric Study of the Reflectivity of the Center of the Martian Disk at Opposition and the Nature of the Violet Layer", Planetary and Space Science, V. 9, March, 1962.

24. Hess, L.L., "A Meteorological Approach to the Question of Water Vapor on Mars and the Mass of the Martian Atmosphere", Astrophysical Journal, 1948.

25. Focas, J.H., 1962, "Seasonal Evaluation of the Fine Structure of the Dark Areas of Mars", Planetary and Space Science, V. 9, July, 1962.

26. Wilson, A.G., "The Atmospheres of Mars and Venus", Publication 944 of the National Academy of Sciences - The National Research Council.

27. Kaplan, L.D., "On the Kiess, Karrer, and Kiess Interpretation of Planetary Spectra", in Studies of the Physical Properties of the Moon and Planets, Quarterly Technical Progress Report (3), Contract R.M. 2769 JPL, The Rand Corporation, p. 62, 1961.

28. Sinton, W.M., "An Upper Limit to the Concentration of NO_2 and N_2O_4 in the Martian Atmosphere", Publs. Astron. Soc., Pacific, 73: 125, 1961.